RAPID COMMUNICATIONS

PHYSICAL REVIEW E VOLUME 47, NUMBER 4 APRIL 1993

Temperature and velocity profiles of turbulent convection in water

A. Tilgner, A. Belmonte, and A. Libchaber*
Physics Department, Jadwin Hall, Princeton University, Princeton, New Jersey 08544
(Received 17 December 1992)

Measurements of temperature and velocity profiles in a convection cell of aspect ratio 1 at a Rayleigh number of 1.1×10^9 and a Prandtl number (Pr) of 6.6 are presented. A large-scale flow persists in the cell. The temperature boundary layer is entirely contained in the viscous boundary layer and the velocity field is smooth on the characteristic length scale of temperature variations. The core of the cell is stably stratified. Most of the heat transported between the plates is carried by the general circulation and does not traverse the core of the cell. Comparison is made with observations at Pr=0.7.

PACS number(s): 47.27.Te, 47.27.Nz

Convection experiments spanning several decades of Rayleigh number (Ra) at a Prandtl number (Pr) of 0.7 in a cell of aspect ratio 1 have revealed a turbulent regime (commonly called "hard turbulence") in which measured quantities scale with Ra above $Ra=4\times10^7$ [1]. For example, the Nusselt number (Nu) is found to vary as $Ra^{2/7}$. This contradicts an earlier theory which assumes that the thermal boundary layer is marginally stable [2]. Consequently, a model [3] was proposed in which the cell is divided into a thermal boundary layer and a central region, separated by a mixing zone. Dimensional arguments then accounted for the measured Nu-Ra dependence. Later experimentation revealed a large-scale flow persistent up to the highest Rayleigh numbers investigated [4]. This large-scale flow was explicitly taken into account by a recent theory [5] which reproduces all experimental observations. The picture emerging from these theories is that there are two distinct boundary layers for the temperature and velocity fields, and that the entire temperature drop occurs within the viscous sublayer. Reference [5] requires in addition that the velocity boundary layer obeys empirically verified scaling laws for shear flows. This theoretical work prompted us to investigate the temperature and velocity fields as a function of height in a convection cell using moveable temperature and velocity probes. The present contribution is aimed at deciding whether two separate boundary layers exist in convection, whereas an ongoing experiment on convection in gas at different pressures will reveal their scaling behaviors.

Our experiments were performed on a cubic cell 18 cm high filled with water [6,7]. The top plate was held at constant temperature by a water cooling system, whereas the bottom plate was electrically heated with constant power. Standard temperatures for the top and bottom plates were 17 and 27 °C, respectively, corresponding to $Ra=1.1\times10^9$ and Pr=6.6 based on material properties at the center of the cell. The sidewalls of the cell were made of glass plates surrounded by a shell of styrofoam.

Temperatures inside the fluid were measured with epoxy coated thermistors [8] 500 μm in size which could be moved vertically under the center of the top plate. The thermistor resistance was recorded by a computer every 50 or 100 ms during measurements which lasted from 15 min to 4 h.

We chose to determine velocity by measuring the distance that electrochemically labeled parcels of fluid travel in a given time [9]. This method is particularly suited to a fluid moving at less than 1 cm/s with inhomogeneous temperature. A *p*H indicator, thymol blue sodium salt, was dissolved at a concentration of 2×10^{-4} per weight in the water. The solution was titrated with 1*N* HCl and NaOH slightly to the acid side of the indicator end point (*p*H 8). The solution is then orange yellow; for a higher *p*H, the solution is dark blue with an absorption maximum at 590 nm. If an electric current passes through two electrodes in the cell, the H^+ ions will be drawn towards the cathode and react to form H_2. The *p*H increases in the neighborhood of the cathode and causes the indicator to change color.

For the velocity measurements, the cathode was the cut end of an insulated 150 μm manganin wire; either plate served as anode. Square pulses of 5 V amplitude and 7/60 s duration were sent through the wire which marked the fluid in the vicinity of the wire tip with blue color. The motion of the marked fluid was almost always uniform for at least 1 s. Note that this labeling method does not introduce any change of density. Furthermore, labeled pieces of fluid lose their color through diffusion after traveling some distance, and the cell does not continuously fill with dye.

The evolution of the labeled fluid was filmed with a CCD camera aimed at the cell perpendicularly to one of the sidewalls. Contrast was enhanced by observing the cell against a diffuser illuminated with a sodium vapor lamp. The video output of the camera was digitized and displayed on a computer screen. One second after a pulse had been sent through the wire, the capture of the video signal was stopped and a human operator recorded the position of the labeled parcel in the frozen image using a mouse. This position could be defined to within 100–200 μm, leading to an uncertainty of 0.1–0.2 mm/s on velocities ranging up to 1 cm/s. Dyed parcels were released every 3 s and a typical time series consisted of 256 or 512 points. From these time series, the vertical velocity component and the horizontal component perpendicular to

 ©1993 The American Physical Society

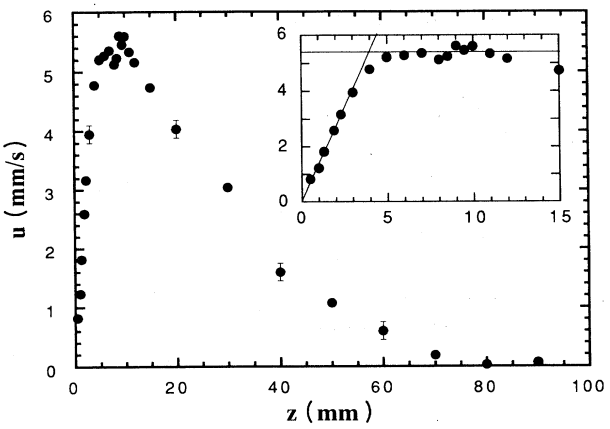

FIG. 1. The horizontal component u of the velocity as a function of distance z from the top plate. The inset is a magnification of the boundary layer region (same data). The center of the cell is at $z=90$ mm. The error on u is ± 0.15 mm/s.

the direction of view of the camera were determined.

The electrode was moved vertically under the center of the top plate in the upper half of the cell. The average horizontal component of the velocity is shown in Fig. 1. The thickness of the viscous layer (defined as the distance at which the extrapolation of the linear part of the profile equals the maximum velocity) is 3.8 ± 0.4 mm. The horizontal velocity reaches a maximum between $z=7$ and 11 mm. The Reynolds number of the shear flow based on this length scale is about 50, whereas the Reynolds number of the large-scale flow is approximately 10^3. The decay of the velocity towards the center is faster than linear, i.e., the core of the cell does not rotate as a solid body. The average vertical component is less than 10% of the horizontal component at all z.

The root-mean-square values of the velocity fluctuations are shown in Fig. 2. For $z>50$ mm, the fluctuations of both components are nearly equal, and larger than the averages.

The temperature profile exhibits a thermal boundary

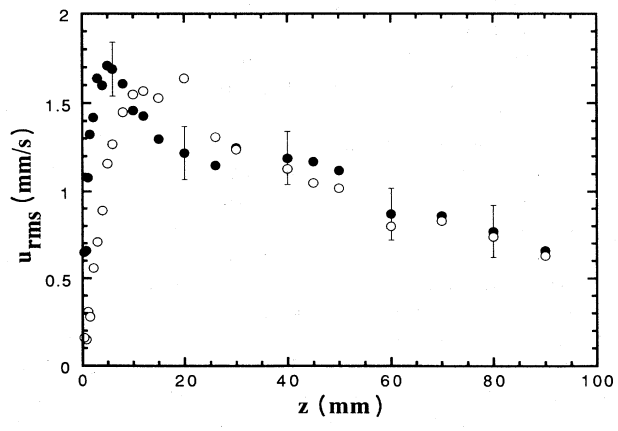

FIG. 2. Root mean square of the velocity fluctuations in the horizontal (dots) and vertical (circles) direction as a function of distance z from the top plate. The error bars are ± 0.15 mm/s.

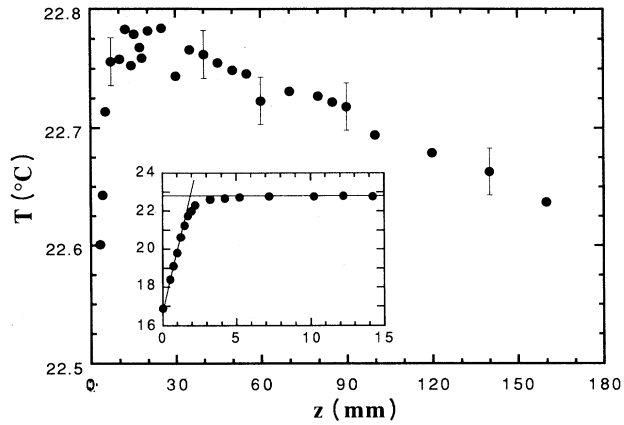

FIG. 3. The mean temperature T as a function of distance z from the top plate. The inset shows the temperature profile in the boundary layer of the top plate. Note that the scale of the ordinate of the main figure is expanded in order to reveal the variation of T in the central region, so that the temperatures of the top and bottom plates (at $z=0$ and 180 mm, respectively) are off scale. The error on T is 0.02 °C.

layer of 1.9 ± 0.3-mm thickness (Fig. 3), defined according to the same procedure used for the viscous boundary layer. The mean temperature reaches a local extremum somewhere between $z=10$ and 30 mm. A weakly stabilizing stratification exists beyond that height (with a mean gradient of 1.1 ± 0.4 mK/mm) throughout the core of the cell. The total temperature drop within this region corresponds to five times the root mean square of the temperature fluctuations at the center of the cell. The root mean square of the temperature fluctuations is maximum at a distance of 1.5 ± 0.3 mm from the plate (Fig. 4).

Simultaneous measurements of velocity and temperature were performed at distances of 3, 25, 70, and 90 mm from the top plate. The thermistor was placed 2 mm away from the electrode such that the line joining the two was perpendicular to the large-scale flow. The velocity at the electrode and the thermistor during the simultaneous measurements can be considered equal because the correlation length of the velocity field exceeds 1 cm [10]. The

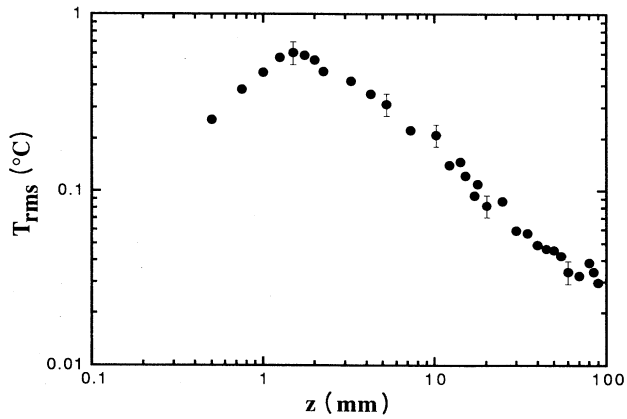

FIG. 4. Root mean square T_{rms} of the temperature fluctuations as a function of distance z from the top plate on logarithmic scales. The error on T_{rms} is $\pm 15\%$.

correlation between temperature and vertical velocity then allows one to calculate the turbulent heat transport and to compare it to the diffusive heat transport through the thermal boundary layer deduced from its temperature profile. We find that the local heat flux at $z=3$ mm approximately equals the heat flux through the boundary layer, whereas at distances of 25 mm or greater, the turbulent heat flux is certainly less than 5% of the heat flux injected by the plate. The actual value is too small to be distinguished from zero within experimental accuracy. The overwhelming part of the heat must therefore be transported close to the cell boundaries by the large-scale flow, whereas the core of the cell contributes negligibly.

We now begin the discussion by summarizing the spatial structure of the velocity field, which we separate into a boundary-layer region and a central region. The latter extends from $z \approx 50$ mm to the center and is characterized by average velocities smaller than the velocity fluctuations, whereas average velocities in the former are larger. Velocity fluctuations vary by a factor of 3 in going from the boundary layer to the center of the cell, and are anisotropic in the boundary-layer region. Visualization is a useful supplement to the quantitative measurements and gives a vivid impression of two distinct regions in the velocity field (Fig. 5). In the central 20% of the cell, the fluctuations of both measured velocity components are equal, vary little in space, and exceed the average speeds by at least an order of magnitude, suggesting that a homogeneous and isotropic velocity field is a suitable approximation for this part of the cell.

Most remarkably, the fluid in the core of the cell is stably stratified. We attribute this inversion to the presence of a large-scale flow. The time necessary to move fluid from the center of one plate to the center of the other plate is twice the size of the cell divided by the speed of the large-scale flow, i.e., 60 s. This time should be compared to the characteristic time for thermalization of the fluid carried by the large-scale flow. Assuming that the heat injected by a plate is transported in a layer of a thickness of about 1 cm (as suggested by the heat flux measurement), and that the heat exchange between this layer and the rest of the cell occurs through diffusion, we obtain a thermalization time of 600 s. According to this estimate, fluid arrives in the vicinity of the opposite plate without being thermalized by the core fluid and may cause a temperature inversion [11]. Efficient heat exchange then occurs at the downstream edges of the plates, where buoyancy dominates, and most plumes are emitted and mix with the fluid carried in the general circulation.

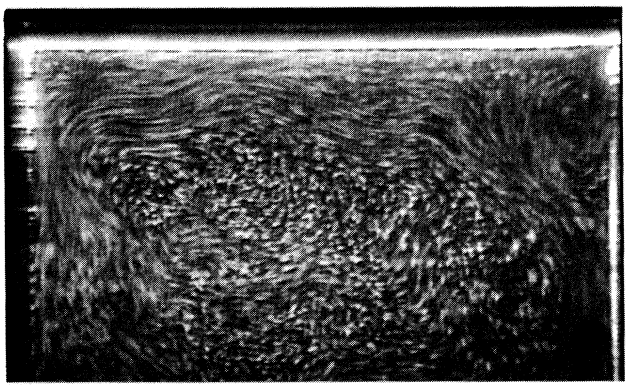

FIG. 5. Streak image obtained by seeding the water with tracer particles and illuminating the cell with a 2-mm-thick sheet of laser light at right angles to the direction of view. Exposure time was 2 s. The bright scattering along the top and sides of the picture comes from the cell boundaries. The bottom plate is outside the field of view.

Let us next consider the boundary-layer region. Two distinct boundary layers exist for the temperature and velocity fields. The assumption of a thermal boundary layer entirely contained in a viscous sublayer is justified. Within the thermal boundary layer, the rms of the temperature fluctuations increases with the distance from the plate because velocity fluctuations also increase and more effectively stir the fluid. The maximum of the temperature fluctuations is expected at the distance at which the velocity fluctuations are largest within the region of largest mean temperature gradient, i.e., at the edge of the thermal boundary layer. This distance is therefore an alternative measure for the thickness of the thermal boundary layer. Beyond this distance, plumes ejected from the boundary layer into the bulk lose through diffusion their temperature contrast with the core fluid as they move through the cell, thus leading to a decrease of the rms of temperature fluctuations with distance.

Turbulent shear flows near a wall are expected to exhibit a viscous sublayer and a region in which the mean velocity varies as the logarithm of the distance to the wall. Observations of velocity boundary layers at high Reynolds number could be fitted by a succession of a linear and logarithmic part [12]. In the present flow, the distance between the edge of the viscous sublayer and the point of maximum velocity is too small for us to decide whether an intrinsically logarithmic profile follows the linear region. The fact that the Reynolds number is only 50 in the shear layer of this convection cell is surprising. It indicates that the main source of turbulence is the instabilities associated with the thermal boundary layer (plumes) or the instabilities of the large-scale flow. The dynamics of this boundary layer can therefore be expected to be different from a pure shear flow near a wall. Thus the logarithmic law, at least with the constants used in Ref. [5], is inappropriate.

We now turn to a comparison with results obtained at lower Pr. Preliminary results from a gas convection cell at room temperature ($\mathrm{Pr}=0.7$ and $\mathrm{Ra}=10^9$) show that the Reynolds number of the velocity boundary layer is 500, with typical velocities for the large-scale flow of 5–10 cm/s, corresponding to a Reynolds number (Re) based on the size of the cell of about 10^4. Also, no gradient of the mean temperature was discernible in the core of this cell, i.e., the total variation of temperature outside the thermal boundary layers is certainly less than the rms of the fluctuations at the center. Concerning the heat transport, it has been estimated for a helium cell at low temperatures that the amount of heat carried by the large-scale flow is of the same order as the heat going

through the center.

We will discuss in turn the two major trends that are observed when Pr is lowered at constant Ra: The heat transport through the center increases and the Reynolds numbers rise. We can rationalize the first observation by noting that at lower Pr, the heat diffusion from a plate into the turbulent region outside the viscous layer is more important. Therefore, more heat escapes the large-scale flow at lower Pr and a larger fraction of the heat exchange goes through the central region. Likewise, the portion of the large-scale flow moving along the sidewalls thermalizes more quickly and will possibly not cause a temperature inversion.

Second, a lower Pr leads to a larger Re. The convective motion at low Pr is dominated by inertia; the fluid is more effective in converting the applied temperature difference into kinetic energy and the flow is more turbulent. A higher Re also means a larger inertial range, since the Kolmogorov length decreases. In this water experiment, we never observed a clearly developed power law in the temperature power spectrum as was seen in a helium cell at the same Ra [1,4].

The Re for the large-scale flow in the water experiment is of the order of 10^3. This is the Re at which the onset of hard turbulence was observed at $Pr=0.7$ [4]. It is generally believed that the presence of the large-scale flow is responsible for the various signatures of the hard turbulence regime. A change of convective behavior may be expected at a Re at which the dynamics of the large-scale flow becomes turbulent and dominated by inertia, which may well happen at $Re\approx 10^3$. We therefore feel that at $Ra=10^9$, we observe just the onset of the hard turbulence region for $Pr=6.6$ [13].

This work was supported by NSF Grant No. DMR 8722714. A.T. gratefully acknowledges support of a NATO grant attributed by the "Deutscher Akademischer Austauschdienst."

---

*Also at NEC Research Institute, 4 Independence Way, Princeton, NJ 08540.

[1] F. Heslot, B. Castaing, and A. Libchaber, Phys. Rev. A **36**, 5870 (1987).

[2] L. N. Howard, J. Fluid Mech. **17**, 405 (1963); W. V. R. Malkus, Proc. R. Soc. London, Ser. A **225**, 185 (1954).

[3] B. Castaing, G. Gunaratne, F. Heslot, L. Kadanoff, A. Libchaber, S. Thomae, X. Z. Wu, S. Zaleski, and G. Zanetti, J. Fluid Mech. **204**, 1 (1989).

[4] M. Sano, X. Z. Wu, and A. Libchaber, Phys. Rev. A **40**, 6421 (1989).

[5] B. I. Shraiman and E. D. Siggia, Phys. Rev. A **42**, 3650 (1990).

[6] G. Zocchi, E. Moses, and A. Libchaber, Physica A **166**, 387 (1990).

[7] T. Y. Chu and R. J. Goldstein, J. Fluid Mech. **60**, 141 (1973); H. Tanka and H. Miyata, Int. J. Heat Mass Transfer **23**, 1273 (1980); R. Krishnamurti and L. N. Howard, Proc. Natl. Acad. Sci. **78**, 4 (1981); T. H. Solomon and J. P. Gollub, Phys. Rev. A **43**, 6683 (1991); P. Tong and Y. Shen, Phys. Rev. Lett. **69**, 2066 (1992).

[8] Purchased from Thermometrics, Inc., 808 US Highway 1, Edison, NJ 08817.

[9] D. J. Baker, J. Fluid Mech. **26**, 573 (1966).

[10] From visual inspection, the persistance length of streak lines (produced, for instance, by sending a constant current through the electrode) is 1–2 cm. The characteristic length scale for velocity variations in streak images like Fig. 5 (with higher resolution) is in the same range. Visualization of the temperature field in the vicinity of the plates [6] has, however, revealed objects that have a characteristic dimension of the order of the thermal boundary-layer thickness, which is approximately 2 mm. The correlation time of the velocity time series exceeds those of the temperature time series by factors varying from 5 in the boundary layer region to 2 in the center.

[11] The temperature profile has also been measured in a corner of the cell in which the fluid rises. The thermistor was moved vertically at a distance of 1.5 cm from the two sidewalls joining in the corner. The temperatures measured at $z=90$ and 20 mm were 0.28 ± 0.04 and 0.12 ± 0.04 °C above the center temperature, respectively. Note that at $z=20$ mm, the thermistor was in the detachment eddy (visible in the upper right corner in Fig. 5) where fluid from the boundary layer and the large-scale flow mix.

[12] S. J. Kline, W. C. Reynolds, F. A. Schraub, and P. W. Runstadler, J. Fluid Mech. **30**, 741 (1967).

[13] A characteristic feature of the hard turbulence state, the exponential histogram of temperature fluctuations at the center, is indeed observed in the water cell.

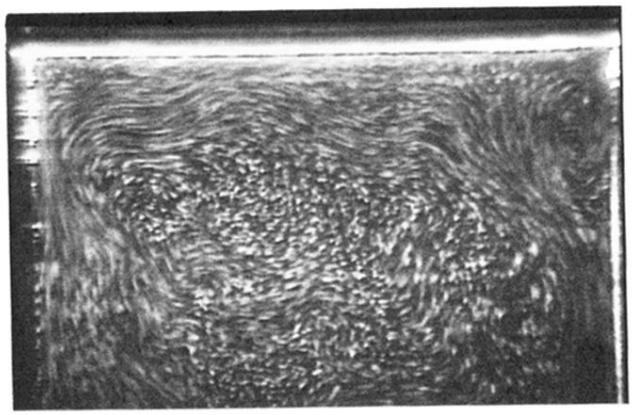

FIG. 5. Streak image obtained by seeding the water with tracer particles and illuminating the cell with a 2-mm-thick sheet of laser light at right angles to the direction of view. Exposure time was 2 s. The bright scattering along the top and sides of the picture comes from the cell boundaries. The bottom plate is outside the field of view.